

Electron Elastic Collision Superconductivity Theory

Hongyuan Ye

hongyy@buaa.edu.cn

[Abstract] The BCS theory explains the superconducting properties of Class I conventional metal and alloy superconductors, but it cannot interpret the superconducting phenomenon of Class II unconventional superconductors. The BCS theory violates Coulomb's law and Heisenberg's uncertainty principle, and its microscopic mechanism of electron-phonon coupling is essentially wrong. Based on the elastic collision theory of Newtonian classical mechanics, this paper proposes the electron elastic collision superconductivity theory, which reveals that the microscopic mechanism of superconducting states is that the free electrons in a current-carrying wire only undergo complete elastic collisions with the atomic lattices, and the current-carrying wire shows zero-resistance superconducting states. The electron elastic collision superconductivity theory proposes the superconducting state free electron critical speed V_C , and theoretically derives the formula for calculating the critical temperature T_C : $2 \Delta_E = 3.7 k_B T_C$. The critical kinetic energy Δ_E of the free electron is equal to the minimum phonon energy $\hbar\gamma$ of the atomic lattice vibration. There is no heat conduction diffusion in the superconducting current-carrying wires, so there are no phonons in the superconductors. The electron elastic collision superconductivity theory interprets the microscopic mechanism of the superconducting state critical temperature T_C , the critical magnetic field H_C , the critical current density j_C , the superconducting state energy gap and the high-pressure superconductor. Unlike Class I conventional superconductors, Class II unconventional superconductors have anisotropic lattices. There are different critical speeds V_C , different critical temperatures T_C and different critical magnetic fields H_C in different directions. Based on the Electron elastic collision superconductivity theory, it is feasible to achieve a zero-resistance superconducting state at normal temperature. Unconventional two-dimensional thin film superconductors and one-dimensional carbon fiber superconductors are the development direction of normal temperature superconductors.

[keyword] BCS theory, Class I conventional superconductor, Class II unconventional superconductor, Coulomb's law, Electron elastic collision superconductivity theory, Free electron critical speed, Critical temperature, Critical magnetic field, Critical current density, Axial critical magnetic field, Radial critical magnetic field.

1. Introduction

In 1911, the Dutch physicist Onnes discovered that mercury suddenly enters a new state with zero-resistance when the temperature drops to around 4.2 K, which is called the superconducting state ^[1].

In 1933, the German physicist Meissner discovered that when a magnetic field is applied to a superconductor, the magnetic field cannot enter the superconductor at all. This completely diamagnetic phenomenon is known as the "Meissner effect". Zero-resistance and

complete diamagnetism are two independent criteria for proving whether a substance is superconductive or not. The superconducting state has a series of critical parameters, such as the critical temperature T_c , the critical magnetic field H_c , the critical current density j_c , etc. Superconducting materials are widely found in metal/non-metal elemental substances, alloys, intermetallic compounds, transition metal oxides, sulfides, selenides, as well as some organic conductors, graphene, C60 structural materials, etc. At present, tens of thousands of superconducting materials have been discovered.

In order to interpret the mechanism of superconductors, a variety of theories have been proposed, the most important is the BCS theory. Based on the electron-phonon coupling interaction, the BCS theory suggests that two electrons with opposite spins in metals can pair up to form a Cooper electron pair, which can move losslessly within the lattices to form superconducting currents. As shown in Figure 1.1. An electron moving within the atomic lattices can attract neighboring positively charged atomic lattices, resulting in a partial distortion of the lattices, and forming a localized region of positive charge. This localized region of positive charge attracts another electron with opposite spin, and pairs with the original electron with a certain binding energy.

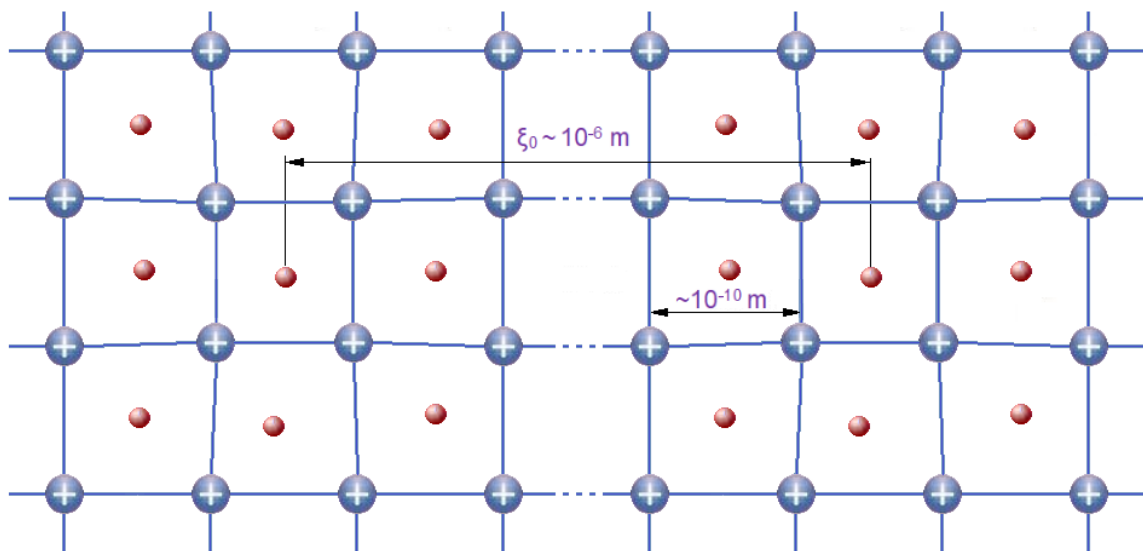


Figure1.1 Microscopic mechanism of the BCS Theory

The BCS theory violates Coulomb's law. Taking conventional metal superconductors as an example, the scale range of an atom is 10^{-10} m, as shown in Figure 1.1. According to Rutherford's alpha particle scattering experiment, Coulomb's law still holds strictly in the scale range of 3×10^{-14} m. If there are paired electrons that are adjacent to each other, there can only be a repulsive force between these two electrons according to Coulomb's law. Two electrons with a repulsive force cannot form a Cooper electron pair. In addition, there is an attractive force between the free electron and the atomic lattice. Since the mass of the atomic lattice is much larger than the mass of the free electron, the result can only be that the free

electron is attracted to the atomic lattice, rather than the atomic lattice being distorted by the electron.

The BCS theory also violates Heisenberg's uncertainty principle. As shown in Figure 1, according to Heisenberg's uncertainty principle, the distance ξ_0 between two electrons in a Cooper pair, which is the BCS coherence length, has a scale range of 10^{-6} m [2], which is equivalent to a distance of approximately 10,000 atomic lattices. At such a long distance, two electrons cannot form a Cooper pair.

The BCS theory contradicts the experimental results. On the one hand, the distortion of atomic lattices cannot logically infer the existence of the Cooper electron pairs. On the other hand, when the temperature decreases and the pressure increases, the activity of the atomic lattices decreases, so the distortion of the atomic lattices decreases. In other words, a decrease in temperature and an increase in pressure are not beneficial for the formation of superconducting states, which is exactly opposite to the experimental results.

The microscopic mechanism of electron-phonon coupling in the BCS theory is essentially wrong. The vibration of the atomic lattices produces phonons, which have quantum properties and the smallest phonon energy is $h\nu$ [3] [4] [5]. When the temperature drops to near absolute zero, the energy of the lattice vibration also approaches zero. In addition, there is no heat conduction diffusion in the superconducting current-carrying wires. Therefore, there are no phonons in the superconductors, and there must be no electron-phonon coupling.

The BCS theory cannot interpret the superconducting phenomenon of Class II unconventional superconductors. According to the BCS theory, the critical temperature of superconductors cannot be higher than 40K, but the critical temperature of unconventional superconductors is much higher than 40K, such as copper oxide superconductors, whose critical temperature can be as high as more than 100K. With high-pressure, even for conventional superconductors, their critical temperature also can be higher than 40K.

2. Preliminary knowledge

2.1 Elastic collisions, inelastic collisions, and completely inelastic collisions

According to Newtonian classical mechanics, the collisions of two elastic objects can be divided into elastic collisions (completely elastic collisions), inelastic collisions and completely inelastic collisions. Without loss of generality, there are two elastic small balls on the ideal smooth plane XOY, with masses of m_1 and m_2 . The mass m_1 is much smaller than m_2 , and the ball with mass m_2 is stationary. There are four springs inside these two small balls to represent their elastic characteristics. As shown in Figures 2.1a, 2.1b and 2.1c.

2.1.1 Elastic collisions

As shown in Figure 2.1a, the elastic ball with mass m_1 collides with the stationary elastic ball with mass m_2 at a speed of V_{11} . During the collision, the springs inside the two elastic

balls are only elastically deformed, not plastically deformed. The kinetic energy of the ball with mass m_1 is only converted to elastic potential energy. After the collision, the two elastic balls are separated. The speed of the ball with mass m_1 is V_{12} , the ball with mass m_2 remains stationary, and the springs inside these two balls return to their original shape before the collision. According to the conservation of energy, the speeds of the small ball with mass m_1 before and after collision are equal; that is, $V_{11} = V_{12}$. Furthermore, the incident angle θ_{11} and the reflection angle θ_{12} of the ball with mass m_1 are equal; that is, $\theta_{11} = \theta_{12}$. The above collision of two small balls is called an elastic collision, or completely elastic collisions.

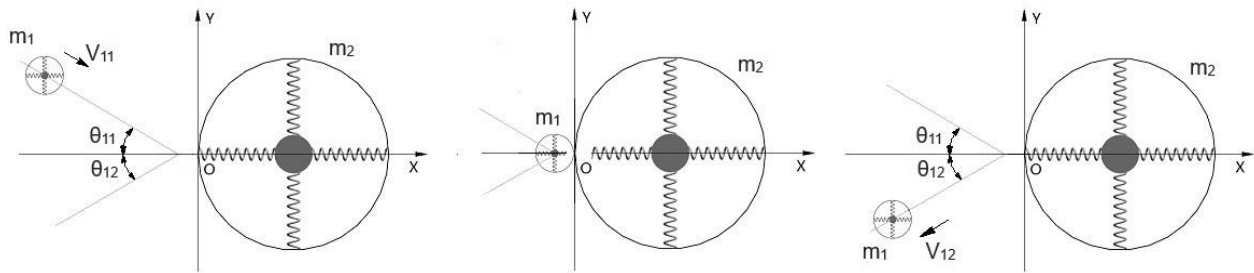


Figure 2.1a Elastic collisions

2.1.2 Inelastic collisions

The speed of the elastic ball with mass m_1 is increased, and it collides with the stationary ball with mass m_2 at a speed of V_{21} , as shown in Figure 2.1b. During the collision, the springs inside the two elastic balls are both elastically and plastically deformed. The kinetic energy of the ball with mass m_1 is partly converted to the elastic potential energy of the springs and partly converted to the plastic deformation of the springs. After the collision, the two elastic balls are separated, the speed of the ball with mass m_1 is V_{22} , and the plastic deformation of the spring cannot be recovered. According to the conservation of energy, the speed of the small ball with mass m_1 after the collision is smaller than the speed before the collision; that is, $V_{22} < V_{21}$. The above collision of two small balls is called an inelastic collision.

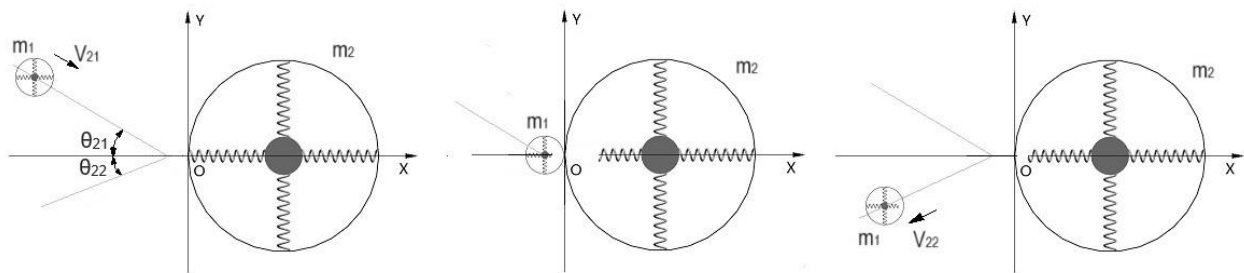


Figure 2.1b Inelastic collisions

2.1.3 Completely inelastic collisions

The speed of the elastic ball with mass m_1 is continually increased, and the ball collides with the stationary ball with mass m_2 at a speed of V_{31} , as shown in Figure 2.1c. During the collision, the springs inside the two elastic balls are both severely plastically deformed, and the kinetic energy of the ball with mass m_1 is completely converted to the plastic deformation of the springs. After the collision, the speed of the ball with mass m_1 is 0, that is, the ball with

mass m_1 and the ball with mass m_2 stick together and remain stationary. The above collision of two small balls is called a completely inelastic collision.

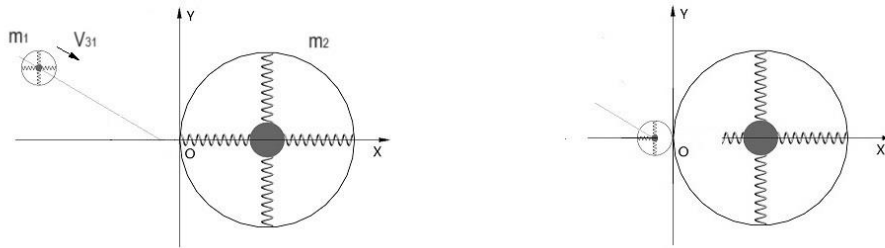


Figure 2.1c Completely inelastic collisions

In the process of above collisions, if the incident angle is zero, that is, the small ball with mass m_1 and the small ball with mass m_2 collide concentrically. Let the incident speed of small ball with mass m_1 increase from low to high. When the speed of small ball with mass m_1 is V_c , the plastic deformation of the small ball with mass m_1 and small ball with mass m_2 begins to occur during the collision, that is, the elastic collision of the two small balls begins to transition to inelastic collision, the speed V_c is called the critical speed of small ball elastic collision.

2.2 The movement of free electrons within a current-carrying wire

In general, taking copper current-carrying wire as an example, the number of free electrons per unit in copper is $n_e=8.5 \times 10^{28}m^{-3}$, and the charge amount of an electron $q_e=1.6 \times 10^{-19}C$. Let the cross-sectional area of the copper wire be $S = 1.0 \text{ mm}^2 = 1.0 \times 10^{-6} \text{ m}^2$, the current passing through the copper wire is $I=1.0A$, and the directional speed of electrons in the wire is V_{eE} driven by the electric field. Then according to the definition, the current:

$$I = q_e n_e S V_{eE} \quad (2-1)$$

From formula (2-1), the current density passing through the copper wire:

$$j = q_e n_e V_{eE} \quad (2-2)$$

From formula (2-1), the directional speed of electrons:

$$V_{eE} = I / (q_e n_e S) \quad (2-3)$$

$$V_{eE} = 1.0 / (1.6 \times 10^{-19} \times 8.5 \times 10^{28} \times 1.0 \times 10^{-6})$$

$$V_{eE} = 7.4 \times 10^{-5} \text{ m/s}$$

The directional speed of electrons V_{eE} is $7.4 \times 10^{-5} \text{ m/s}$. However, according to the classical free electron theory of metals [7], the average kinetic energy of the Irregular thermal motion of free electrons in a metal conductor is as follows:

$$m_e V_{eT}^2 / 2 = 3 k_B T / 2 \quad (2-4)$$

Then the average speed of the Irregular thermal motion of free electrons is:

$$V_{eT} = (3 k_B T / m_e)^{1/2} \quad (2-5)$$

where $k_B = 1.38 \times 10^{-23} \text{ J/K}$, which is the Boltzmann constant; $m_e = 0.91 \times 10^{-30} \text{ kg}$ is the electron mass; and T is the thermodynamic temperature. If $t = 27 \text{ }^\circ\text{C}$, then $T = 300 \text{ K}$. Substituting these values into equation (2-5), it can be obtained:

$$V_{eT} = 1.17 \times 10^5 \text{ m/s}$$

In summary, in a current-carrying wire at normal temperature, the speed of free electrons is a combination of massive Irregular thermal motion with a very small directional movement. The random thermal speed of free electrons in the current-carrying wire is huge, and the thermal speed of the atomic lattices is also quite large.

3. Electron elastic collision superconductivity theory

From the above analysis, it can be concluded that at normal temperature, without the electric field, the free electrons and the atomic lattices both take high-speed random thermal motion. However, the high-speed thermal motion is relative to its zero-point position, and the zero-point position is unchanged. The free electron at high-speed thermal motion is confined within a fixed atomic lattice, then the collision between the electron and the adjacent atomic lattice is mainly an elastic collision, which will not produce a lot of heat. Driven by an applied electric field, the free electrons move directionally to form a current. Although the directional movement speed of free electrons is very small, which is in the scale range of 10^{-5} m/s, the free electrons pass through different atomic lattices. A considerable number of collisions between the electrons and adjacent atomic lattices are inelastic collisions, which generates a large amount of heat.

When the temperature drops to near absolute zero, the speed of Irregular thermal motion of free electrons and atomic lattices approaches zero. The relative speed between the free electrons and the atomic lattices is in the scale range of 10^{-5} m/s. The collisions at such low-speed can only be elastic collisions. Before and after the collisions, the energy of the free electrons and the atomic lattices does not change. The current-carrying wire is in a zero-resistance superconducting state. Based on the above analysis, the following conclusion can be drawn.

Electron elastic collision superconductivity theory: The microscopic mechanism of superconducting states is that during the directional motion of the free electrons in the current-carrying wire, only elastic collisions occur between the free electrons and atomic lattices. Before and after collisions, the energy of the free electrons and the atomic lattices does not change. The current-carrying wire displays zero-resistance superconducting states.

In the superconducting states, elastic collisions also occur between two free electrons, and kinetic energy exchange occurs between them, but the total kinetic energy of the two free electrons remains constant. The free electrons can be regarded as an elastic microsphere with a negative charge. Although the total charge of an atomic lattice carries positive charges, protons with a positive charge are all concentrated in a narrow space located at the core of the atomic lattice, and electrons with negative charges are all located

on the periphery of the atomic lattice. The core of the atomic lattice shows positive electric field characteristics, and the periphery of the atomic lattice shows negative electric field characteristics.

As shown in Figure 3.1, the red indicates a negative electric field, and the blue indicates a positive electric field. The free electron is a small red elastic ball, and the depth of the red color represents the intensity of the negative electric field. The core of the atomic lattice is a blue central ball, and the depth of blue color represents the intensity of the positive electric field. The outer periphery of the blue central ball is a red spherical shell. The radius of the blue central ball is R_C , and the thickness of the red outer spherical shell is ΔD_C . The region of the atomic lattice within the radius R_C is the positive electric field, and the region outside the radius R_C is the negative electric field.



Figure 3.1 The electric field characteristics of electrons and atomic lattices

During the collisions between free electrons and atomic lattices, if the collision only occurs in the red peripheral region of the lattices, it is an elastic collision and the current-carrying wire shows zero-resistance superconducting states. If the free electrons break through the red peripheral region of the lattices ΔD_C and reach the blue region within R_C , the collision at that time is an inelastic collision. Before and after collision, the energy of the free electrons and the atomic lattices changes, and the current-carrying wire shows normal resistance states. R_C is called the lattice critical elastic radius, and ΔD_C is called the lattice critical elastic thickness.

The below takes the monovalent aluminum ion (Al^+) as an example to prove that the periphery of the atomic lattice has negative electric field characteristics ^[8]. The monovalent aluminum ion nucleus has 13 protons and 12 electrons. To simplify the analysis, 12 electrons are evenly distributed in the same circular orbit with radius r_0 , as shown in Figure 3.2.

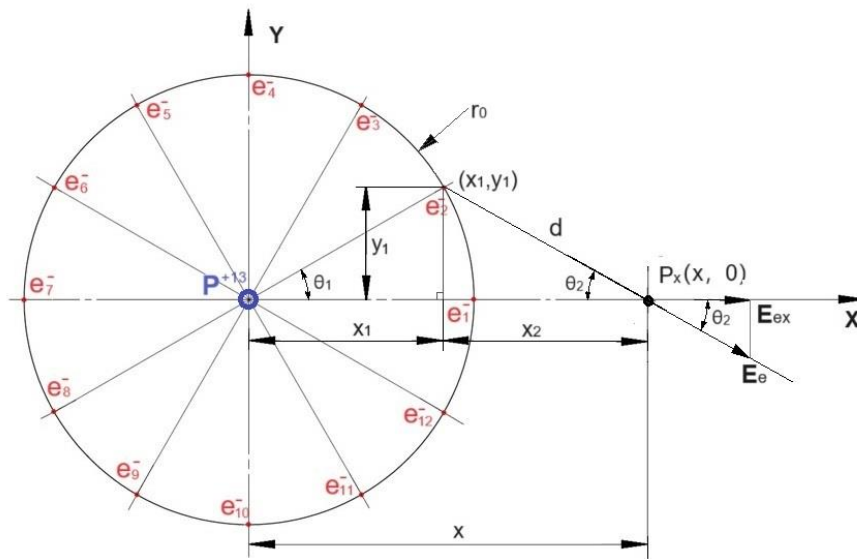


Figure 3.2 Electric field characteristics of monovalent Aluminum Ions

Let $r_0 = 0.75 \times 10^{-10} \text{ m}$, take a point P_x on the x-axis of the periphery of the monovalent aluminum-ion lattice, and $x = 1.25 \times 10^{-10} \text{ m}$. According to the geometric relationships in Figure 5, the following mathematical formulas can be obtained:

$$x_1 = r_0 \cos\theta_1$$

$$y_1 = r_0 \sin\theta_1$$

$$x_2 = x - x_1$$

$$d^2 = y_1^2 + x_2^2$$

$$\cos\theta_2 = x_2 / d$$

The electric field intensity produced by electron e at the point P_x is:

$$E_e = -k q_e / d^2$$

where $k = 9.0 \times 10^9 \text{ N m/C}^2$, $q_e = 1.6 \times 10^{-19} \text{ C}$. The component of E_e on the x-axis is:

$$E_{ex} = E_e \cos\theta_2$$

According to the above formulas, Table 1 can be obtained.

Table 1 The electric field intensity generated by the 12 electrons at point P_x

| | θ_1 (deg) | x_1 (10^{-10}m) | y_1 (10^{-10}m) | x_2 (10^{-10}m) | d (10^{-10}m) | $\cos\theta_2$ | E_e (V/m) | E_{ex} (V/m) |
|-------|---------------------|---------------------------------|---------------------------------|---------------------------------|-------------------------------|----------------|------------------------|------------------------|
| e_1 | 0 | 0.750 | 0.000 | 0.500 | 0.500 | 1.000 | -57.6×10^{10} | -57.6×10^{10} |
| e_2 | 30 | 0.650 | 0.375 | 0.600 | 0.708 | 0.847 | -28.7×10^{10} | -24.3×10^{10} |
| e_3 | 60 | 0.375 | 0.650 | 0.875 | 1.090 | 0.803 | -12.1×10^{10} | -9.72×10^{10} |
| e_4 | 90 | 0.000 | 0.750 | 1.250 | 1.458 | 0.857 | -6.77×10^{10} | -5.80×10^{10} |
| e_5 | 120 | -0.375 | 0.650 | 1.625 | 1.750 | 0.928 | -4.70×10^{10} | -4.36×10^{10} |
| e_6 | 150 | -0.650 | 0.375 | 1.900 | 1.937 | 0.981 | -3.84×10^{10} | -3.77×10^{10} |
| e_7 | 180 | -0.750 | 0.000 | 2.000 | 2.000 | 1.000 | -3.6×10^{10} | -3.60×10^{10} |
| e_8 | 210 | -0.650 | -0.375 | 1.900 | 1.937 | 0.981 | -3.84×10^{10} | -3.77×10^{10} |
| e_9 | 240 | -0.375 | -0.650 | 1.625 | 1.750 | 0.928 | -4.70×10^{10} | -4.36×10^{10} |

| | | | | | | | | |
|-----------------|-----|-------|--------|-------|-------|-------|--------------------------|--------------------------|
| e ₁₀ | 270 | 0.000 | -0.750 | 1.250 | 1.458 | 0.857 | -6.77 x 10 ¹⁰ | -5.80 x 10 ¹⁰ |
| e ₁₁ | 300 | 0.375 | -0.650 | 0.875 | 1.090 | 0.803 | -12.1 x 10 ¹⁰ | -9.72 x 10 ¹⁰ |
| e ₁₂ | 330 | 0.650 | -0.375 | 0.600 | 0.708 | 0.847 | -28.7 x 10 ¹⁰ | -24.3 x 10 ¹⁰ |

Due to the symmetrical and uniform distribution of the 12 electrons, the component of their total electric field intensity on the y-axis is zero. From Table 1, the total electric field intensity generated by the 12 electrons of a monovalent aluminum ion (Al⁺) at point P_x is:

$$\begin{aligned}
 E_{\text{exAll}} &= -57.6 - (24.3+9.72+5.80+4.36+3.77) - 3.60 - (24.3+9.72+5.80+4.36+3.77) \\
 &= -57.6 - 47.95 - 3.60 - 47.95 \\
 &= -157.1 \times 10^{10} \text{ V/m}
 \end{aligned}$$

The nucleus has 13 protons, and the electric field intensity generated by the nucleus at point P_x is:

$$\begin{aligned}
 E_{\text{px}} &= 13 k q_e / x^2 \\
 &= 119.8 \times 10^{10} \text{ V/m}
 \end{aligned}$$

The total electric field intensity generated by the monovalent aluminum ion (Al⁺) at point P_x is:

$$\begin{aligned}
 E_{\text{All}} &= E_{\text{px}} + E_{\text{exAl}} \\
 &= 119.8 \times 10^{10} - 157.1 \times 10^{10} \\
 E_{\text{All}} &= -37.3 \times 10^{10} \text{ V/m}
 \end{aligned}$$

where "-" indicates that there is negative electric field characteristics at point P_x, that is, the periphery of the atomic lattice has a negative electric field. In order to further prove that the periphery of the atomic lattice has a negative electric field, the next step will be to build a more rigorous mathematical model based on the quantum free electron theory, the band theory and the Schrödinger wave function.

The free electron is an elastic small ball with a negative electric field, and the periphery of the atomic lattice is also a weak negative electric field, there is a repulsive force between the free electron and the lattice. In the superconducting states, the free electron moves closer to the atomic lattice at a low-speed V_e, and the free electron decelerates under the electric field repulsive force. The free electron and the lattice undergo elastic collision only within the red peripheral region of the lattice. After the collision, the free electron accelerates away from the lattice under the electric field repulsive force, and the free electron accelerates to the original speed V_e. Therefore, before and after the collision between the free electron and the lattice, the speed of the free electron remains the same, and there is no energy exchange between the free electron and the lattice.

When a free electron and an atomic lattice collide concentrically, and the incident speed of the free electron increases to V_c, the free electron begins to break through the red peripheral region of the lattice and reaches the blue region within R_c. The speed V_c is called the free electron critical speed. The kinetic energy of the free electron corresponding to the critical speed V_c is called the free electron critical kinetic energy Δ_E.

There is a repulsive force between the free electrons and atomic lattices. In addition, the free electrons are uniformly distributed among the atomic lattices. Therefore, the atomic lattices do not undergo inward contraction or outward expansion distortion, as shown in Figure 3.3.

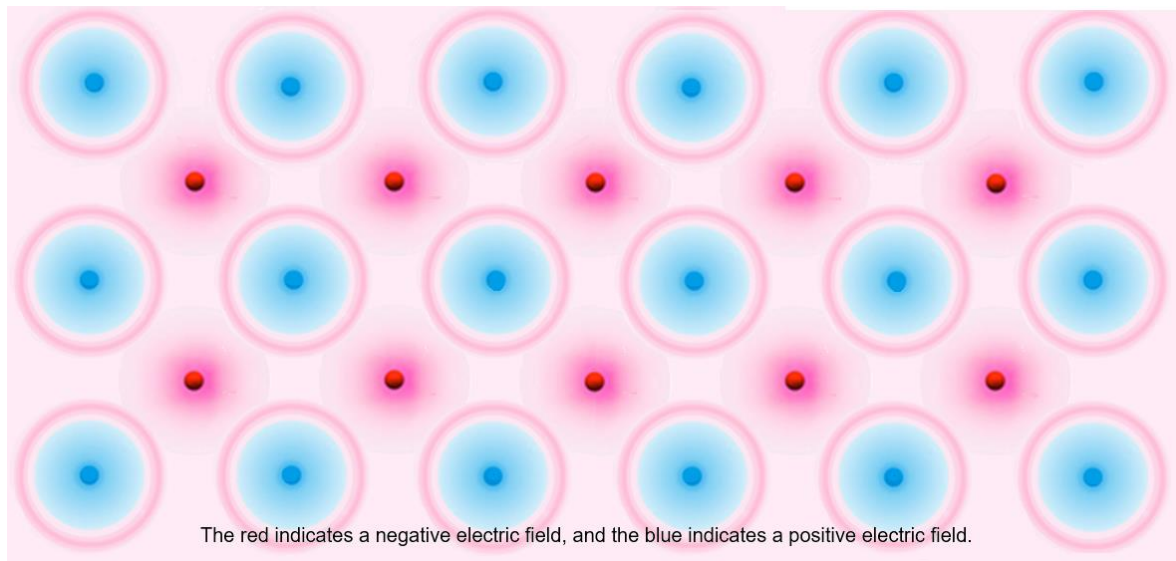


Figure 3.3 Atomic lattice structure without distortion

The important reason for the widespread acceptance of BCS theory is the famous formula for calculating the critical temperature T_C [6].

$$2 \Delta = 3.53 k_B T_C \quad (3-1)$$

The energy gap Δ and critical temperature T_C are both experimental measurement values. The energy gap Δ can be measured through experiments such as far-infrared absorption, electron tunnel experiments, and critical field experiments.

Table 2 shows the experimental measurement values of $2\Delta/k_B T_C$ [7][8]. From Table 2, it can be concluded that with different experimental methods, there is a significant difference between the theoretical values of coefficient 3.53 and the experimental values. Even with the same experimental method but different experimental groups, the experimental coefficients are still significantly different.

Table 2 Experimental measurement values of $2\Delta/k_B T_C$.

| Superconducting material | Experimental group | Far-infrared absorption | Electron tunnel | Critical field |
|--------------------------|--------------------|-------------------------|-----------------|----------------|
| Al | I | | 4.2 ± 0.6 | 3.53 |
| | II | | 2.5 ± 0.3 | |
| | III | | 3.37 ± 0.1 | |
| Sn | I | 3.6 | 3.46 ± 0.1 | 3.61 |
| | II | | 3.10 ± 0.05 | 3.57 |
| | III | | 2.8 – 4.06 | |
| In | I | 4.1 | 3.63 ± 0.1 | 3.65 |

| | | | | |
|----|----|------|-----------------|------|
| | II | | 3.45 ± 0.07 | |
| Pb | I | 4.14 | 4.29 ± 0.04 | 3.95 |
| | II | | 4.38 ± 0.01 | |
| Hg | I | 4.6 | 4.6 ± 0.05 | 3.95 |
| Nb | I | 2.8 | 3.84 ± 0.06 | 3.65 |
| | II | | 3.6 | |

Equation (3-1) is an approximate calculation formula derived based on the quantum free electron theory and experimental measurement data. The theoretical derivation does not require the concept of the Cooper electron pairs; there is no relationship between Cooper electron pairs and equation (3-1).

Based on the electron elastic collision superconductivity theory and the classical free electron theory, one can also derive the formula for calculating the critical temperature T_C . Assuming that the critical speed of the free electron is V_C and the average speed is V_{Te} , the critical speed V_C is the maximum speed. Let $V_{Te} = k_e V_C$, the proportional coefficient $k_e < 1$. The critical temperature T_C is corresponding to the critical speed V_C . From formula (2-4), the relationship between V_C and T_C is as follows:

$$m_e (k_e V_C)^2 / 2 = 3 k_B T_C / 2 \quad (3-2)$$

The critical kinetic energy of a free electron at the critical speed V_C is:

$$\Delta E = m_e V_C^2 / 2 \quad (3-3)$$

From equations (1-4) and (1-5), it can be concluded that

$$2 \Delta E = (3/k_e^2) k_B T_C \quad (3-4)$$

If the free electron moves directionally at a constant speed, its average speed is equal to the maximum speed, then $k_e = 1$. If the free electron is only moving thermally and the speed is a sinusoidal function, then $k_e = 0.637$. In the superconducting state, the main motion of free electrons is the directional constant motion. Take $k_e = 0.9$, then it can be obtained from equation (1-6):

$$2 \Delta E = 3.7 k_B T_C \quad (3-5)$$

Equations (3-5) and (3-1) are approximate experimental formulas, and their proportional coefficients are 3.70 and 3.53, respectively, which are within the experimental error.

During the collision of free electrons and atomic lattices, the critical kinetic energy ΔE of the electrons can be converted in whole or in part into the energy of the atomic lattices. If the vibrational energy of the atomic lattices reaches the minimum energy $h\nu$ of the phonon, the vibrational energy of the lattices can be diffused outward with phonons. Before and after the collision, the energy of both the free electrons and the atomic lattices changes, and the

current-carrying wire changes from a superconducting state to a resistive state. The critical kinetic energy ΔE of the electron is equal to the minimum energy $h\nu$ of the phonon.

In equation (3-5), the physical concept of ΔE is much clearer, and ΔE is also easier to measure experimentally. An experimental measurement method for the critical kinetic energy ΔE of electrons is discussed below. As shown in Figure 3.2, the experiment utilizes a superconducting thin film with a thickness on the nanometer scale. This thin film is placed in a vacuum insulation box. There is an electron emission gun on the left side of the vacuum insulation box, and there are electron speed measurement sensors on the left and right sides of the box. The vacuum insulation box is also equipped with a temperature sensor for measuring the temperature of the superconducting thin film

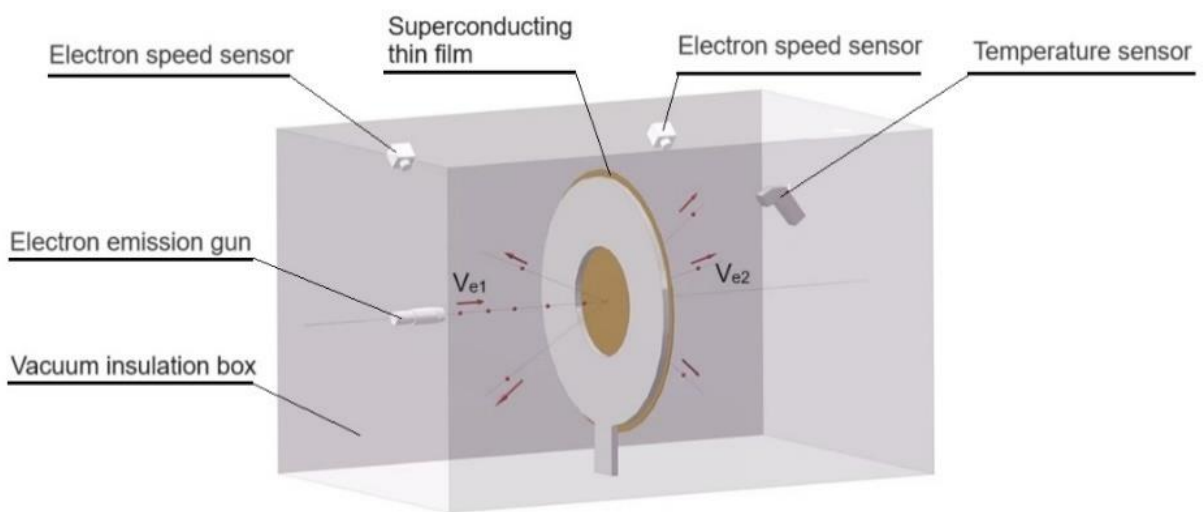


Figure 3.2 Experiment for the measurement of critical kinetic energy ΔE

In the experiment, first, the superconducting thin film is cooled to T_{C1} , which is below the critical temperature T_C . The electrons emitted by the electron gun move toward the superconducting thin film at a speed of V_{e1} . After the collision between the electrons and the superconducting thin film, the speed of the electrons is V_{e2} . Some electrons are reflected to the left side of the vacuum box, while others pass through the superconducting thin film and enter the right side of the vacuum box. When the electrons move at a low speed of V_{e1} , the collisions between the electrons and the superconducting thin film are elastic collisions, and the speed of electrons stays the same after the collisions; that is, $V_{e1} = V_{e2}$. At the same time, the temperature of the superconducting thin film measured using the temperature sensor remains unchanged. The speed of the electrons is increased to V_{C1} , and after the collisions between electrons and superconducting thin film, the speed of some electrons decreases. This means that the collisions between electrons and superconducting thin film are inelastic collisions. At the same time, the temperature of the superconducting thin film measured using the temperature sensor is increased. T_{C1} and V_{C1} are substituted into equations (3-3) and (3-5) to verify these two equations. Different T_{C2} and T_{C3} values are used, and the corresponding V_{C2} and V_{C3} are obtained with experiments, further verifying that the Boltzmann constant k_B

stays the same near absolute zero.

Before and after a collision of the free electron and lattice, the momentum of the free electron changes. However, the collisions between the free electron and lattices occur randomly, the number of collisions is large, and the number of free electrons in the current-carrying wire is also very large. Based on the macroscopic statistics of random collisions, the momentum of the free electrons is conserved, that is, the direction of the movement of the free electrons remains unchanged.

4. The Interpretation of Superconducting States by Electron Elastic Collision Superconductivity Theory

The microscopic mechanism of the superconducting states is that only elastic collisions occur between free electrons and atomic lattices, and no energy exchange occurs between free electrons and lattices. The current-carrying wire displays zero-resistance superconducting states.

4.1 Free electron critical speed V_C

Within a current-carrying wire, the free electron critical speed V_C is the essence of the superconducting states. When the speed of free electrons relative to the atomic lattices is lower than V_C , only elastic collisions occur between the free electrons and the atomic lattices, the current-carrying wire presents zero-resistance superconducting states. The free electron critical speed V_C is the addition of the directional speed V_{eE} and the random thermal speed V_{eT} of the free electron. The free electron critical speed is:

$$V_C = V_{eE} + V_{eT} \quad (4-1)$$

For a free electron at critical speed V_C , its corresponding critical kinetic energy:

$$\Delta_E = m_e V_C^2 / 2$$

The critical kinetic energy Δ_E of the electron is equal to the minimum energy $h\nu$ of the phonon.

4.2 The critical temperature T_C , the critical magnetic field H_C , and the critical current density j_C

The critical temperature T_C , the critical magnetic field H_C and the critical current density j_C are the three important critical parameters of the superconducting states.

When the temperature drops to the critical temperature T_C , the current-carrying wire enters a zero-resistance superconducting state. The irregular thermal motion speed of free electrons and atomic lattices decreases with the temperature decreasing. The critical temperature T_C corresponds to the free electron critical speed V_C . The critical temperature T_C is the macroscopic statistical representation of superconductivity, and the critical speed V_C is the microscopic mechanism of superconductivity.

When a magnetic field is applied axially along a superconducting current-carrying wire, a vortex current is generated radially in the current-carrying wire to counteract the external magnetic field, so as to keep the magnetic induction intensity within the superconductor at zero. The applied magnetic field will produce a Lorentz magnetic field force on the free electrons in the current-carrying wire, and the directional speed of the free electron is superimposed on a vortex current speed V_{eB} , which is proportional to the applied magnetic field. When the applied magnetic field reaches the critical magnetic field H_C , the superimposed vortex current speed V_{eB} makes the speed of the free electrons reach the critical speed V_C , and the current-carrying wire enters the normal resistance states. The microscopic mechanism of the critical magnetic field H_C is that the speed of the free electrons is superimposed on a vortex current speed V_{eB} .

Experiments also show that the superconducting state of a current-carrying wire is limited by the current density. When the current density reaches a certain critical current density j_C , the current-carrying wire recovers from the zero-resistance superconducting state to the normal-resistance state. According to formula (2-2), the directional motion speed V_{eE} of free electrons is directly proportional to the current density. When the current density reaches the critical current density j_C , the corresponding free electron speed also reaches the critical speed V_C , and the current-carrying wire enters the normal-resistance state. The microscopic mechanism of the critical current density j_C is the increasing of the directional motion speed of free electrons.

In summary, the microscopic mechanism of the critical temperature T_C , the critical magnetic field H_C and the critical current density j_C of superconductivity is that the free electrons reach at the critical speed V_C .

4.3 Gap Energy

Far infrared absorption is a way to experimentally measure the energy gap Δ . The cavity is made of superconducting materials, and the far-infrared radiation is introduced into the cavity through a light pipe, and a far-infrared radiation detection element is placed in the cavity. Far-infrared photons can be detected by the detection element after multiple reflections in the cavity. When the frequency of far-infrared light $\gamma < \gamma_g$, the energy of far-infrared photons is smaller, the collision between far-infrared photons and superconducting wall lattices of the cavity is a completely elastic collision, there is no energy exchange between far-infrared photons and superconducting wall lattices. The superconducting wall does not absorb any far-infrared photon, all far-infrared photons are retained in the cavity, and a large radiation signal can be detected by the detection element. When the radiation frequency is $\gamma \geq \gamma_g$, the energy of far-infrared photons is large enough, the collision between far-infrared photons and superconducting wall lattices is an inelastic collision, there is energy exchange between far-infrared photons and superconducting wall lattices. The

superconducting wall absorbs a large number of far-infrared photons, only part of the far-infrared photons is retained in the cavity, the signal received on the detection element decreases rapidly. The frequency γ_g is called the critical frequency, and the critical photon energy with the frequency γ_g is called the energy gap of the superconductor:

$$\Delta = h \gamma_g$$

Where $h = 6.626 \times 10^{-34}$ J·s, which is Planck's constant.

4.4 Class II unconventional superconductor

Metal, alloy and compound superconductors are usually referred to as class I conventional superconductors, and high-temperature superconductors such as copper oxide superconductors, iron-based superconductors, organic superconductors, and two-dimensional superconductors are called class II unconventional superconductors. The lattice structure of conventional superconductors is relatively simple, and it is generally face-centered, body-centered, hexagonal dense pile, quadrangular crystal system, rhomboidal crystal system, etc., they all have isotropic, zero resistance and completely diamagnetic superconducting properties. Based on the dynamical theory of lattices and the experimental data of conventional superconductors, Bardeen, Cooper and Schrieffer put forward the famous BCS theory. The BCS theory states that the critical temperature cannot be higher than 40 K at normal atmospheric pressure.

In 1986, Swiss scientists Bernorz and Miller discovered a barium-lanthanum-copper oxide superconductor, which critical temperature was higher than 35 K. Later, through the efforts of scientists from many countries, the superconducting critical temperature was soon increased to 90K. The high-temperature unconventional superconductor is a huge challenge to the BCS theory. Class II unconventional superconductors have complex lattice structures and generally have anisotropic superconducting properties. Fig. 4.1a shows the lattice structure of $\text{YBa}_2\text{Cu}_3\text{O}_7$ with a critical temperature T_c at 90K; Fig. 4.1b shows the lattice structure of $\text{Bi}_2\text{Sr}_2\text{Ca}_2\text{Cu}_3\text{O}_{10+y}$ with a critical temperature T_c up to 110K.

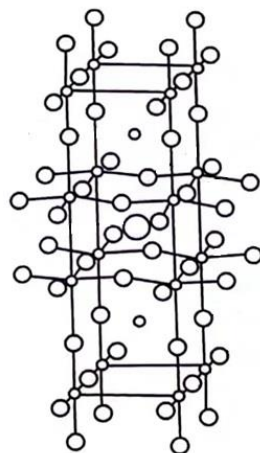


Figure 4.1a $\text{YBa}_2\text{Cu}_3\text{O}_7$

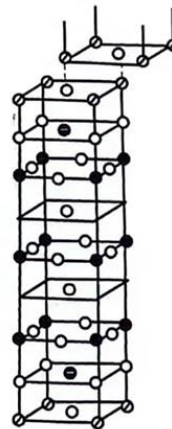


Figure 4.1b $\text{Bi}_2\text{Sr}_2\text{Ca}_2\text{Cu}_3\text{O}_{10+y}$

Class II unconventional superconductor generally includes different atomic lattices, and the atomic lattices are unevenly distributed. Class II unconventional superconductor can be simplified as long cylindrical lattice. If the direction of the long cylindrical lattice is the same as that of the current-carrying wire, on the one hand, the long cylindrical lattice provides a smooth channel for the axial flow of free electrons, and on the other hand, unconventional superconductor lattice usually has a low Irregular thermal motion even at higher temperature. For these two reasons, class II unconventional superconductors have a high free electron critical speed V_C , and their corresponding critical temperature T_C is also higher.

For Class I conventional superconductors, when the applied external magnetic field $H_a < H_C$, the superconductor shows complete diamagnetism, and when $H_a = H_C$, the superconductor returns to a normal resistance state. Class II unconventional superconductors have a lower critical magnetic field H_{C1} and an upper critical magnetic field H_{C2} , and $H_{C1} < H_{C2}$. When the applied external magnetic field $H_a < H_{C1}$, the superconductor shows a complete diamagnetic phenomenon. When the applied magnetic field $H_a = H_{C1}$, the magnetic field begins to enter the superconductor, but the superconductor maintains zero-resistance state. When the applied magnetic field $H_a > H_{C1}$, the magnetic field enters the superconductor more and more, but the superconductor still maintains zero-resistance state. When the applied magnetic field $H_a = H_{C2}$, the superconductor returns to the normal resistance state, and the magnetic field completely enters the conductor.

The following is an in-depth analysis of the reasons why the critical magnetic field of Class II superconductors differs from that of Class I superconductors

Class II unconventional superconductor can be simplified as long cylindrical lattice. As shown in Figure 4.2, the direction of the long cylindrical lattice is the same as that of the current-carrying wire, which provides a smooth channel for the axial flow of free electrons, Therefore, class II superconductors have a higher free electron critical speed in the axial direction, which is the axial critical speed V_{C2} . Corresponding to the axial critical speed V_{C2} is the axial critical magnetic field, which is the upper critical magnetic field H_{C2} .

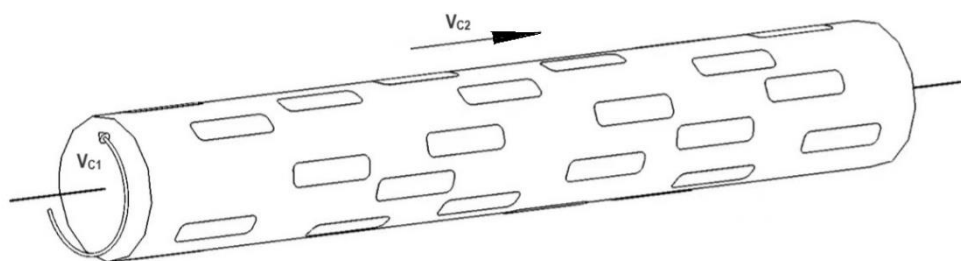


Figure 4.2 Anisotropy of a class II superconductor

The applied external magnetic field H_a generates vortex currents in the radial direction of the current-carrying wire, and the radial flow of free electrons is not as smooth as the axial flow. Class II superconductors have a lower free electron critical speed in the radial direction,

which is the radial critical speed V_{C1} . Corresponding to the radial critical speed V_{C1} is the radial critical magnetic field, which is the lower critical magnetic field H_{C1} . The axial critical speed is greater than the radial critical speed, that is, $V_{C2} > V_{C1}$. The axial critical magnetic field is greater than the radial critical magnetic field, that is, $H_{C2} > H_{C1}$.

When the applied external magnetic field $H_a < H_{C1}$, the radial speed of the free electrons $V_a < V_{C1}$. The axial and radial flow of the free electrons both remain in zero-resistance states, and the superconductor shows a complete diamagnetism. When the applied magnetic field $H_a = H_{C1}$, the radial speed of the free electrons $V_a = V_{C1}$. The radial flow of the free electrons begins to enter a normal-resistance state, the vortex current cannot completely offset the applied magnetic field H_{C1} , then the magnetic field begins to enter the superconductor, but the axial flow of free electrons remains in a zero-resistance state.

When the applied magnetic field $H_a > H_{C1}$, the radial speed of the free electrons $V_a > V_{C1}$. The magnetic field entering the superconductor increases with the increasing of the applied magnetic field H_a , but the axial flow of the free electrons still remains in a zero-resistance state. When the applied magnetic field $H_a = H_{C2}$, the axial speed of the free electrons also reaches the critical speed V_{C2} , the axial flow and radial flow of the free electrons both enter the normal resistance states, the superconductor returns to the normal resistance states, and the magnetic field completely enters the conductor.

To sum up, the zero-resistance state and the complete diamagnetism are not two independent criteria for superconducting states. The essence of superconducting state is the zero-resistance. The diamagnetism is due to the fact that the magnetic field generated by the vortex current can offset the external applied magnetic field, so that the superconductor shows a complete diamagnetic phenomenon. For class II unconventional superconductors, when $H_{C1} < H_a < H_{C2}$, the superconductor is still in a zero-resistance state, but the magnetic field generated by the vortex current cannot completely offset the external applied magnetic field, so the external magnetic field enters the superconductor.

A verification experiment is proposed for the above diamagnetic theoretical analysis of superconducting states. As shown in Figure 4.3, coating a superconducting thin film on a silicon cylinder, and the thin film material can be either Class I conventional superconductor or Class II unconventional superconductor, the thickness of the superconducting thin film ranges from 0.1 nm to 1.0 nm. Along the axis of the silicon cylinder, a longitudinal groove is opened on the superconducting thin film, so that the superconducting film coated on the silicon cylinder cannot form a radial vortex current, and the external applied magnetic field can completely enter the superconducting thin film.

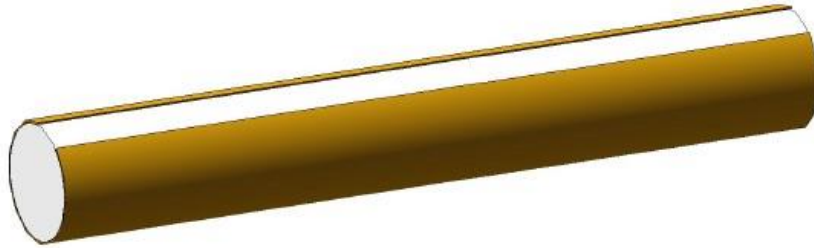


Figure 4.3 Experiment of diamagnetic properties of superconducting thin film

4.5 High pressure superconductor

Temperature and pressure are the two most important environmental parameters. Similar to the decreasing in temperature, the increasing of ambient pressure also will reduce the random thermal movement speed of free electrons and lattices. Even at a higher temperature, the free electron speed remains below the critical speed V_C . A high-pressure environment is beneficial for the formation of superconducting states.

5. Summary and discussion

The BCS theory violates Coulomb's law and Heisenberg's uncertainty principle, and its microscopic mechanism of electron-phonon coupling is essentially wrong.

Based on the elastic collision theory of Newtonian classical mechanics, this paper proposes the electron elastic collision superconductivity theory, which reveals that the microscopic mechanism of superconducting states is that the free electrons in a current-carrying wire only undergo complete elastic collisions with the atomic lattices. The current-carrying wire displays zero-resistance superconducting states.

In a superconductor, two free electrons collide elastically, the kinetic energy will be exchanged between them, but the total kinetic energy of the two free electrons remains constant. In fact, when free electrons and atomic lattices collide elastically, the kinetic energy will also be exchanged between them, but this kinetic energy is less than the minimum energy of the phonon, so that the phonon cannot be generated. Based on macroscopic statistics, in the superconducting states, the total kinetic energy of the atomic lattices remains constant, and the total kinetic energy of the free electrons remains constant.

According to the electron elastic collision superconductivity theory, it is theoretically feasible to achieve a zero-resistance superconducting state at normal temperature. The irregular thermal movement of the silicon lattice is very small. By infiltrating metal nano-atoms, this silicon-based conductor is a promising high-temperature superconducting material. Another feasible normal-temperature superconducting material is carbon, which is easy to

form different atomic lattices, two-dimensional carbon film and one-dimensional carbon fiber are the development direction of normal temperature superconductors.

The electron elastic collision superconductivity theory reveals that free electrons and atomic lattices only undergo complete elastic collisions in superconductors. Can this theory be extended to the propagation of light quanta in glass media? Light quantum propagates in a glass medium, and it only undergoes a complete elastic collision with the glass medium. Light quantum can propagate without loss in the glass medium.

REFERENCES

- [1] Yuheng Zhang, The Physics of Superconductors (3rd Edition), University of Science and Technology of China Press, Hefei, 2009
- [2] Yidong Huang, Fundamentals of Solid-State Physics (1st Edition), Tsinghua University Press, Beijing, 2022
- [3] Quanxi Cao et al., Fundamentals of Solid-State Physics (1st Edition), Xidian University Press, Xian, 2008
- [4] Charles Kittel, Introduction to Solid State Physics (Eighth Edition), Chemical Industry Press, Beijing, 2005
- [5] Jian Zhou, Qifeng Liang, Fundamentals of First-Principles Materials Calculations, Science Press, Beijing, 2019
- [6] Wangjun Feng, Jianfeng Dai, College Physics (Volume 1, 2nd Edition), Science Press, Beijing, 2021:
- [7] Daniel A. Fleisch, A Student's Guide to the Schrödinger Equation (1st Edition), China Machine Press, Beijing, 2022
- [8] Richard P. Feynman et al., The Feynman Lectures on Physics (Volume 3), The New Millennium Edition, Shanghai Science & Technical Publishers, Shanghai, 2020